Investigation of the Behavior of an Interface Crack between Two Half-Planes of Orthotropic Functionally Graded Materials by Using a New Method*

Zhen-Gong ZHOU**, Biao WANG** and Li-Jian YANG**

In this paper, the problem of a crack along an interface between inhomogeneous orthotropic media is solved by using a new method, named the Schmidt method. To make the analysis tractable, it is assumed that the Poisson's ratios of the mediums are constant and the material modulus varies exponentially with coordinate parallel to the crack. By use of the Fourier transform, the problem can be solved with the help of two pairs of dual integral equations in which the unknown variables are the jumps of the displacements across the crack. To solve the dual integral equations, the jumps of the displacements across the crack surfaces are expanded in a series of Jacobi polynomials. Numerical examples are provided to show the effects of the length of the crack and the parameter describing the functionally graded materials upon the stress intensity factor of the cracks. When the material properties are continuous across the crack line, the numerical results are the same as those obtained so far. When the material properties are not continuous across the crack line, an approximate solution of the interface crack problem is given under the assumptions that the effect of the crack surface overlapping very near the crack tips is negligible. Contrary to the previous solution of the interface crack, it is found that the stress singularities of the present interface crack solution are similar with ones for the ordinary crack in homogenous orthotropic materials.

Key Words: Elasticity, Interface Crack, Orthotropic Materials, Functionally Graded Materials, Schmidt Method, Dual Integral Equations

1. Introduction

The analysis of functionally graded materials (FGMs) has become a subject of increasing importance motivated by a number of potential benefits achievable from the use of such novel materials in a wide range of modern technological practices. The major advantages of graded materials, especially in elevated temperature environments, stem from the tailoring capability to produce a gradual variation of its thermomechanical properties in the spatial domain(1). In particular, the use of a graded material as interlayers between bonded media is one of the highly effective and promising applications in eliminating various shortcoming resulting from stepwise property mismatch inherent in piecewise homogeneous composite media(2)–(4).

From the fracture mechanics viewpoint, the presence of a graded interlayer would play an important role in determining the crack driving forces and fracture resistance parameters. In an attempt to address the issues pertaining to the fracture analysis of bonded media with such transitional interfacial properties, a series of solutions to certain crack problems was obtained by Erdogan and his associates(5)–(7). Among them there are the solutions for a crack in the non-homogeneous interlayer bounded by dissimilar homogeneous media(5); and for a crack at the interface between homogeneous and non-homogeneous materials(6), (7). Similar problems of delamination or an interface crack between a functionally graded coating and a substrate were considered in Refs. (8) – (10). The dynamic crack problem for non-homogeneous composite materials was considered in Ref. (11) but authors considered the FGM layer as a multi-layered homogeneous medium. The crack problem in FGM layers under thermal stresses was studied by Edrogen and Wu(12). They considered an unconstrained elastic layer under statically self-equilibrating

* Received 20th November, 2003 (No. 03-5142)
** Center for Composite Materials and Electro-Optics Technology Center, Harbin Institute of Technology, P.O. Box 1247, Harbin 150001, P.R. China.
E-mail: zhouzhg@hit.edu.cn

thermal or residual stresses.

In this paper, the problem in Ref. (13) is reworked using a somewhat different approach, named the Schmidt method[(14),(15)]. As discussed in Ref. (13), it is assumed that the Poisson's ratios $\nu_{ik}^{(j)}$ $(i,k = 1,2,3,\ j = 1,2)$ of the mediums are constants and the material modulus $\mu_{ik}^{(j)}$, $E_i^{(j)}$ $(i,j,k = 1,2)$ varies exponentially with coordinate parallel to the crack. By use of the Fourier transform technique, the problem can be solved with the help of two pairs of dual integral equations in which the unknown variables are the jumps of the displacements across the crack surfaces. To solve the dual integral equations, the jumps of the displacements across crack surfaces are expanded in a series of Jacobi polynomials. This process is quite different from those adopted in Refs. (1) – (13) and (15) – (20) as mentioned above. However, in the previous works[(5)–(13),(18)–(20)], the unknown variables of dual integral equations are the dislocation density functions. This is the major difference. First, the numerical solutions are obtained for the stress intensity factors when the material properties are continuous along the crack line. The numerical results are similar with that in Ref. (13). Second, the numerical solutions are also obtained when the material properties are not continuous across the crack line under the assumptions that the effect of the crack surface overlapping very near the crack tips is negligible. For this special case (From practical view points, researchers in the field of functionally graded materials will not pay their attention in this case), it is found that the stress singularities of the present interface crack solution are similar with ones for the ordinary crack in homogeneous orthotropic materials[(16),(17)].

2. Formulation of the Crack Problem

It is assumed that there is an interface crack of length $2l$ along the x-axis between two dissimilar orthotropic FGM half-planes $-\infty < x < \infty$, $0 \le y < \infty$ and $-\infty < x < \infty$, $-\infty < y \le 0$ as shown in Fig. 1. As discussed in Refs. (13) and (18), to make the analysis tractable, the elastic constants of the FGM are assumed to be as follows in the global $x-y$ coordinates

$$\mu_{ik}^{(j)} = \mu_{ik0}^{(j)} e^{\beta^{(j)}x},\ E_i^{(j)} = E_{i0}^{(j)} e^{\beta^{(j)}x},\ (j = 1,2;\ i,k = 1,2,3) \tag{1}$$

where $\beta^{(j)}$ is a constant (The superscript $j = 1,2$ corresponds to the upper half plane and the lower half plane throughout this paper.). If $\mu_{120}^{(1)} = \mu_{120}^{(2)}$, $E_{10}^{(1)} = E_{20}^{(2)}$ and $\beta^{(1)} = \beta^{(2)}$, the problem in this paper will return to the same problem as discussed in Ref. (13).

Here, $u^{(j)}(x,y)$ and $v^{(j)}(x,y)$ represent the displacement components in the x- and y-directions, respectively. The constitutive relations for the non-homogeneous material are written as

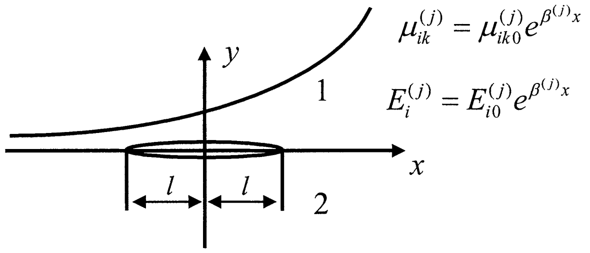

Fig. 1 Geometry of the interface crack between two dissimilar orthotropic functionally graded materials and the variation of the elastic constants $\mu_{ik}^{(j)} = \mu_{ik0}^{(j)} e^{\beta^{(j)}x}$ and $E_i^{(j)} = E_{i0}^{(j)} e^{\beta^{(j)}x}$ $(i,j,k = 1,2)$

$$\sigma_x^{(j)}(x,y) = \mu_{120}^{(j)} e^{\beta^{(j)}x}\left[c_{11}^{(j)}\frac{\partial u^{(j)}}{\partial x} + c_{12}^{(j)}\frac{\partial v^{(j)}}{\partial y}\right],\ (j = 1,2) \tag{2}$$

$$\sigma_y^{(j)}(x,y) = \mu_{120}^{(j)} e^{\beta^{(j)}x}\left[c_{12}^{(j)}\frac{\partial u^{(j)}}{\partial x} + c_{22}^{(j)}\frac{\partial v^{(j)}}{\partial y}\right],\ (j = 1,2) \tag{3}$$

$$\tau_{xy}^{(j)}(x,y) = \mu_{120}^{(j)} e^{\beta^{(j)}x}\left[\frac{\partial u^{(j)}}{\partial y} + \frac{\partial v^{(j)}}{\partial x}\right],\ (j = 1,2) \tag{4}$$

The non-dimensional parameters $c_{ik}^{(j)}$ $(i,k = 1,2,3,\ j = 1,2)$ involved in the above equations are related to the elastic constants by the relations:

$$\begin{aligned}
c_{11}^{(j)} &= E_{10}^{(j)} \Big/ \left[\mu_{120}^{(j)}\left(1 - \nu_{12}^{(j)2} E_{20}^{(j)}/E_{10}^{(j)}\right)\right] \\
c_{22}^{(j)} &= E_{20}^{(j)} \Big/ \left[\mu_{120}^{(j)}\left(1 - \nu_{12}^{(j)2} E_{20}^{(j)}/E_{10}^{(j)}\right)\right] = c_{11}^{(j)} E_{20}^{(j)}/E_{10}^{(j)} \\
c_{12}^{(j)} &= \nu_{12}^{(j)} E_{20}^{(j)} \Big/ \left[\mu_{120}^{(j)}\left(1 - \nu_{12}^{(j)2} E_{20}^{(j)}/E_{10}^{(j)}\right)\right] = \nu_{12}^{(j)} c_{22}^{(j)} \\
&= \nu_{21}^{(j)} c_{11}^{(j)},\ (j = 1,2)
\end{aligned} \tag{5}$$

for generalized plane stress, and by

$$\begin{aligned}
c_{11}^{(j)} &= E_{10}^{(j)}\left(1 - \nu_{23}^{(j)}\nu_{32}^{(j)}\right) \Big/ \left(\Delta^{(j)}\mu_{120}^{(j)}\right) \\
c_{22}^{(j)} &= E_{20}^{(j)}\left(1 - \nu_{13}^{(j)}\nu_{31}^{(j)}\right) \Big/ \left(\Delta^{(j)}\mu_{120}^{(j)}\right) \\
c_{12}^{(j)} &= E_{10}^{(j)}\left(\nu_{21}^{(j)} + \nu_{13}^{(j)}\nu_{32}^{(j)} E_{20}^{(j)}/E_{10}^{(j)}\right) \Big/ \left(\Delta^{(j)}\mu_{120}^{(j)}\right) \\
&= E_{20}^{(j)}\left(\nu_{12}^{(j)} + \nu_{23}^{(j)}\nu_{31}^{(j)} E_{10}^{(j)}/E_{20}^{(j)}\right) \Big/ \left(\Delta^{(j)}\mu_{120}^{(j)}\right) \\
\Delta^{(j)} &= 1 - \nu_{12}^{(j)}\nu_{21}^{(j)} - \nu_{23}^{(j)}\nu_{32}^{(j)} - \nu_{31}^{(j)}\nu_{13}^{(j)} - \nu_{12}^{(j)}\nu_{23}^{(j)}\nu_{31}^{(j)} \\
&\quad - \nu_{13}^{(j)}\nu_{21}^{(j)}\nu_{32}^{(j)},\ (j = 1,2)
\end{aligned} \tag{6}$$

for plane strain. $\nu_{ik}^{(j)}$ $(j = 1,2;\ i,k = 1,2,3)$ are the Poisson's ratio and are taken to be constant; owing to the fact its variation within a practical range has an insignificant influence on the value of the near-tip driving for fracture[(1)–(3)].

In this paper, we just consider the generalized plane stress problem. The equations of equilibrium of the orthotropic FGMs, in the absence of body forces, may be expressed as follows:

$$\begin{aligned}
&c_{11}^{(j)}\frac{\partial^2 u^{(j)}}{\partial x^2} + \frac{\partial^2 u^{(j)}}{\partial y^2} + \left(1 + c_{12}^{(j)}\right)\frac{\partial^2 v^{(j)}}{\partial x \partial y} \\
&\quad + \beta^{(j)}\left(c_{11}^{(j)}\frac{\partial u^{(j)}}{\partial x} + c_{12}^{(j)}\frac{\partial v^{(j)}}{\partial y}\right) = 0,\ (j = 1,2)
\end{aligned} \tag{7}$$

$$\frac{\partial^2 v^{(j)}}{\partial x^2}+c_{22}^{(j)}\frac{\partial^2 v^{(j)}}{\partial y^2}+\left(1+c_{12}^{(j)}\right)\frac{\partial^2 u^{(j)}}{\partial x\partial y}$$
$$+\beta^{(j)}\left(\frac{\partial u^{(j)}}{\partial y}+\frac{\partial v^{(j)}}{\partial x}\right)=0,\ (j=1,2) \tag{8}$$

3. Solution

The system of above governing equations is solved, using the Fourier integral transform technique to obtain the general expressions for the displacement components as

$$\begin{cases} u^{(1)}(x,y)=\dfrac{1}{2\pi}\displaystyle\int_{-\infty}^{\infty}\sum_{j=1}^{2}A_j(s)e^{-\lambda_j(s)y}e^{-isx}ds \\ v^{(1)}(x,y)=\dfrac{1}{2\pi}\displaystyle\int_{-\infty}^{\infty}\sum_{j=1}^{2}m_j(s)A_j(s)e^{-\lambda_j(s)y}e^{-isx}ds \end{cases} \tag{9}$$

$$\begin{cases} u^{(2)}(x,y)=\dfrac{1}{2\pi}\displaystyle\int_{-\infty}^{\infty}\sum_{j=3}^{4}A_j(s)e^{-\lambda_j(s)y}e^{-isx}ds \\ v^{(2)}(x,y)=\dfrac{1}{2\pi}\displaystyle\int_{-\infty}^{\infty}\sum_{j=3}^{4}m_j(s)A_j(s)e^{-\lambda_j(s)y}e^{-isx}ds \end{cases} \tag{10}$$

and from Eqs. (2) – (4), the stress components are obtained as

$$\begin{cases} \sigma_y^{(1)}(x,y)=\dfrac{\mu_{120}^{(1)}e^{\beta^{(1)}x}}{2\pi}\displaystyle\int_{-\infty}^{\infty}\sum_{j=1}^{2}\left[-isc_{12}^{(1)}-c_{22}^{(1)}m_j(s)\lambda_j(s)\right]A_j(s)e^{-\lambda_j(s)y}e^{-isx}ds \\ \tau_{xy}^{(1)}(x,y)=\dfrac{\mu_{120}^{(1)}e^{\beta^{(1)}x}}{2\pi}\displaystyle\int_{-\infty}^{\infty}\sum_{j=1}^{2}\left[-\lambda_j(s)-im_j(s)s\right]A_j(s)e^{-\lambda_j(s)y}e^{-isx}ds \end{cases} \tag{11}$$

$$\begin{cases} \sigma_y^{(2)}(x,y)=\dfrac{\mu_{120}^{(2)}e^{\beta^{(2)}x}}{2\pi}\displaystyle\int_{-\infty}^{\infty}\sum_{j=3}^{4}\left[-isc_{12}^{(2)}-c_{22}^{(2)}m_j(s)\lambda_j(s)\right]A_j(s)e^{-\lambda_j(s)y}e^{-isx}ds \\ \tau_{xy}^{(2)}(x,y)=\dfrac{\mu_{120}^{(2)}e^{\beta^{(2)}x}}{2\pi}\displaystyle\int_{-\infty}^{\infty}\sum_{j=3}^{4}\left[-\lambda_j(s)-im_j(s)s\right]A_j(s)e^{-\lambda_j(s)y}e^{-isx}ds \end{cases} \tag{12}$$

where s is the transform variable, A_j $(j=1,2,3,4)$ are arbitrary unknowns.

$\lambda_j(s)$ $(j=1,2)$ are the roots of the following characteristic equation

$$c_{22}^{(1)}\lambda^4-\left[s^2\left(c_{11}^{(1)}c_{22}^{(1)}-c_{12}^{(1)2}-2c_{12}^{(1)}\right)+is\beta^{(1)}\left(c_{11}^{(1)}c_{22}^{(1)}-2c_{12}^{(1)}-c_{12}^{(1)2}\right)+\beta^{(1)2}c_{12}^{(1)}\right]\lambda^2+c_{11}^{(1)}s^2\left(s+i\beta^{(1)}\right)^2=0 \tag{13}$$

and $m_j(s)$ $(j=1,2)$ are expressed for each root $\lambda_j(s)$ $(j=1,2)$ as

$$m_j(s)=\frac{-c_{11}^{(1)}s^2+\lambda_j^2(s)-is\beta^{(1)}c_{11}^{(1)}}{\lambda_j(s)\left[-is\left(1+c_{12}^{(1)}\right)+\beta^{(1)}c_{12}^{(1)}\right]},\ (j=1,2) \tag{14}$$

$\lambda_j(s)$ $(j=3,4)$ are the roots of the following characteristic equation

$$c_{22}^{(2)}\lambda^4-\left[s^2\left(c_{11}^{(2)}c_{22}^{(2)}-c_{12}^{(2)2}-2c_{12}^{(2)}\right)+is\beta^{(2)}\left(c_{11}^{(2)}c_{22}^{(2)}-2c_{12}^{(2)}-c_{12}^{(2)2}\right)+\beta^{(2)2}c_{12}^{(2)}\right]\lambda^2+c_{11}^{(2)}s^2\left(s+i\beta^{(2)}\right)^2=0 \tag{15}$$

and $m_j(s)$ $(j=3,4)$ are expressed for each root $\lambda_j(s)$ $(j=3,4)$ as

$$m_j(s)=\frac{-c_{11}^{(2)}s^2+\lambda_j^2(s)-is\beta^{(2)}c_{11}^{(2)}}{\lambda_j(s)\left[-is\left(1+c_{12}^{(2)}\right)+\beta^{(2)}c_{12}^{(2)}\right]},\ (j=3,4) \tag{16}$$

The roots may be obtained as

$$\lambda_1(s)=\sqrt{\frac{\alpha^{(1)}(s)+\sqrt{\alpha^{(1)2}(s)-4\gamma^{(1)}(s)c_{22}^{(1)}}}{2c_{22}^{(1)}}},\quad \lambda_2(s)=\sqrt{\frac{\alpha^{(1)}(s)-\sqrt{\alpha^{(1)2}(s)-4\gamma^{(1)}(s)c_{22}^{(1)}}}{2c_{22}^{(1)}}} \tag{17}$$

$$\lambda_3(s)=-\sqrt{\frac{\alpha^{(2)}(s)+\sqrt{\alpha^{(2)2}(s)-4\gamma^{(2)}(s)c_{22}^{(2)}}}{2c_{22}^{(2)}}},\quad \lambda_4(s)=-\sqrt{\frac{\alpha^{(2)}(s)-\sqrt{\alpha^{(2)2}(s)-4\gamma^{(2)}(s)c_{22}^{(2)}}}{2c_{22}^{(2)}}} \tag{18}$$

where

$$\alpha^{(1)}(s)=s^2\left(c_{11}^{(1)}c_{22}^{(1)}-c_{12}^{(1)2}-2c_{12}^{(1)}\right)+is\beta^{(1)}\left(c_{11}^{(1)}c_{22}^{(1)}-2c_{12}^{(1)}-c_{12}^{(1)2}\right)+\beta^{(1)2}c_{12}^{(1)},\quad \gamma^{(1)}(s)=c_{11}^{(1)}s^2\left(s+i\beta^{(1)}\right)^2,$$

$$\alpha^{(2)}(s)=s^2\left(c_{11}^{(2)}c_{22}^{(2)}-c_{12}^{(2)2}-2c_{12}^{(2)}\right)+is\beta^{(2)}\left(c_{11}^{(2)}c_{22}^{(2)}-2c_{12}^{(2)}-c_{12}^{(2)2}\right)+\beta^{(2)2}c_{12}^{(2)},\quad \gamma^{(2)}(s)=c_{11}^{(2)}s^2\left(s+i\beta^{(2)}\right)^2.$$

From Eqs. (9) – (12), it can be seen that there are four unknown constants (in Fourier space they are functions of s), i.e., A_j, $j=1,2,3,4$, which can be determined from the following boundary conditions:

$$\sigma_y^{(1)}(x,0)=\sigma_y^{(2)}(x,0)=-\sigma_0(x),$$
$$\tau_{xy}^{(1)}(x,0)=\tau_{xy}^{(2)}(x,0)=-\tau_0(x),\quad |x|\le l \tag{19}$$
$$\sigma_y^{(1)}(x,0)=\sigma_y^{(2)}(x,0),\ \tau_{xy}^{(1)}(x,0)=\tau_{xy}^{(2)}(x,0),\quad |x|>l \tag{20}$$
$$u^{(1)}(x,0)=u^{(2)}(x,0),\ v^{(1)}(x,0)=v^{(2)}(x,0),\quad |x|>l \tag{21}$$

where $\sigma_0(x)$ and $\tau_0(x)$ are known functions.

Let $f_i(x)$ $(i=1,2)$ be the jumps of the displacements across the crack surfaces defined as follows:

$$f_1(x)=u^{(1)}(x,0)-u^{(2)}(x,0) \tag{22}$$
$$f_2(x)=v^{(1)}(x,0)-v^{(2)}(x,0) \tag{23}$$

In the solution of such problem, it is obvious that some unsurmountable mathematical difficulties will be encountered and have to be simplified with the parameter $\beta^{(i)}$ $(i=1,2)$. In this paper, it is decided to assume $\beta^{(1)}=\beta^{(2)}=\beta$. Applying the Fourier transforms and the boundary conditions (19)–(21), it can be obtained

$$[X_1]\begin{bmatrix}A_1(s)\\A_2(s)\end{bmatrix}=[X_2]\begin{bmatrix}A_3(s)\\A_4(s)\end{bmatrix} \tag{24}$$
$$[X_3]\begin{bmatrix}A_1(s)\\A_2(s)\end{bmatrix}-[X_4]\begin{bmatrix}A_3(s)\\A_4(s)\end{bmatrix}=\begin{bmatrix}\bar f_1(s)\\\bar f_2(s)\end{bmatrix} \tag{25}$$

where

$$[X_1]=\begin{bmatrix}\mu_{120}^{(1)}\left[-isc_{12}^{(1)}-c_{22}^{(1)}m_1(s)\lambda_1(s)\right] & \mu_{120}^{(1)}\left[-isc_{12}^{(1)}-c_{22}^{(1)}m_2(s)\lambda_2(s)\right]\\ \mu_{120}^{(1)}[-\lambda_1(s)-im_1(s)s] & \mu_{120}^{(1)}[-\lambda_2(s)-im_2(s)s]\end{bmatrix},$$
$$[X_2]=\begin{bmatrix}\mu_{120}^{(2)}\left[-isc_{12}^{(2)}-c_{22}^{(2)}m_3(s)\lambda_3(s)\right] & \mu_{120}^{(2)}\left[-isc_{12}^{(2)}-c_{22}^{(2)}m_4(s)\lambda_4(s)\right]\\ \mu_{120}^{(2)}[-\lambda_3(s)-im_3(s)s] & \mu_{120}^{(2)}[-\lambda_4(s)-im_4(s)s]\end{bmatrix},$$
$$[X_3]=\begin{bmatrix}1 & 1\\ m_1(s) & m_2(s)\end{bmatrix},\quad [X_4]=\begin{bmatrix}1 & 1\\ m_3(s) & m_4(s)\end{bmatrix}.$$

A superposed bar indicates the Fourier transform. The Fourier transform is defined as follows:

$$\bar f(s)=\int_{-\infty}^{\infty}f(x)e^{isx}dx,\quad f(x)=\frac{1}{2\pi}\int_{-\infty}^{\infty}\bar f(s)e^{-isx}ds \tag{26}$$

By solving four Eqs. (24) and (25) with four unknown functions, substituting the solutions into Eq. (19) and applying the boundary conditions, it can be obtained

$$\sigma_y^{(1)}(x,0)=\frac{e^{\beta x}}{2\pi}\int_{-\infty}^{\infty}\left[d_1(s)\bar f_1(s)+d_2(s)\bar f_2(s)\right]e^{-isx}ds=-\sigma_0(x),\quad 0\le|x|\le l \tag{27}$$
$$\tau_{xy}^{(1)}(x,0)=\frac{e^{\beta x}}{2\pi}\int_{-\infty}^{\infty}\left[d_3(s)\bar f_1(s)+d_4(s)\bar f_2(s)\right]e^{-isx}ds=-\tau_0(x),\quad 0\le|x|\le l \tag{28}$$
$$\int_{-\infty}^{\infty}\bar f_1(s)e^{-isx}ds=0,\quad |x|>l \tag{29}$$
$$\int_{-\infty}^{\infty}\bar f_2(s)e^{-isx}ds=0,\quad |x|>l \tag{30}$$

where $d_1(s)$, $d_2(s)$, $d_3(s)$ and $d_4(s)$ are known functions as follows

$$[X_5]=[X_3]-[X_4][X_2]^{-1}[X_1],\quad \begin{bmatrix}d_1(s) & d_2(s)\\ d_3(s) & d_4(s)\end{bmatrix}=[X_1][X_5]^{-1}$$

To determine the unknown functions $\bar f_1(s)$ and $\bar f_2(s)$, the above two pairs of dual integral Eqs. (27)–(30) must be solved.

4. Solution of the Dual Integral Equations

To solve the problem, the jumps of the displacements across the crack surfaces can be represented by the following series (When the material properties are not continuous along the crack line, as assumption mentioned above, the problem is solved under the assumptions that the effect of the crack surface overlapping very near the crack tips is negligible. These assumptions had been used in Refs. (18)–(20). It can be obtained that the jumps of the displacements across the crack surface are finite, differentiable and continuous functions.):

$$f_1(x)=\sum_{n=0}^{\infty}a_nP_n^{(1/2,1/2)}\left(\frac{x}{l}\right)\left(1-\frac{x^2}{l^2}\right)^{\frac{1}{2}},\quad \text{for}\quad 0\le|x|\le l \tag{31}$$
$$f_1(x)=0,\quad \text{for}\quad |x|>l \tag{32}$$

$$f_2(x)=\sum_{n=0}^{\infty} b_n P_n^{(1/2,1/2)}\left(\frac{x}{l}\right)\left(1-\frac{x^2}{l^2}\right)^{\frac{1}{2}}, \quad \text{for} \quad 0\le|x|\le l \tag{33}$$

$$f_2(x)=0, \quad \text{for} \quad |x|>l \tag{34}$$

where a_n and b_n are unknown coefficients, $P_n^{(1/2,1/2)}(x)$ is a Jacobi polynomial[21]. The phenomenon of the crack surface overlapping near the crack tips will not be included in the series as shown in Eqs. (31) – (34). The Fourier transform of Eqs. (31) – (34) is[22]

$$\bar{f}_1(s)=\sum_{n=0}^{\infty} a_n G_n \frac{1}{s} J_{n+1}(sl), \quad \bar{f}_2(s)=\sum_{n=0}^{\infty} b_n G_n \frac{1}{s} J_{n+1}(sl) \tag{35}$$

$$G_n=2\sqrt{\pi}(-1)^n i^n \frac{\Gamma\left(n+1+\frac{1}{2}\right)}{n!} \tag{36}$$

where $\Gamma(x)$ and $J_n(x)$ are the Gamma and Bessel functions, respectively.

Substituting Eq. (35) into Eqs. (27) – (30), it can be shown that Eqs. (29) – (30) are automatically satisfied. After integration with respect to x in $[-l,x]$, Eqs. (27) and (28) reduce to

$$\frac{1}{2\pi}\sum_{n=0}^{\infty} G_n \int_{-\infty}^{\infty} \frac{i}{s^2}\left[d_1(s)a_n+d_2(s)b_n\right] J_{n+1}(sl)\left[e^{-isx}-e^{isl}\right] ds=-\int_{-l}^{x}\sigma_0(s)e^{-\beta s}ds, \quad 0\le|x|\le l \tag{37}$$

$$\frac{1}{2\pi}\sum_{n=0}^{\infty} G_n \int_{-\infty}^{\infty} \frac{i}{s^2}\left[d_3(s)a_n+d_4(s)b_n\right] J_{n+1}(sl)\left[e^{-isx}-e^{isl}\right] ds=-\int_{-l}^{x}\tau_0(s)e^{-\beta s}ds, \quad 0\le|x|\le l \tag{38}$$

From the relationships[21]

$$\int_0^{\infty}\frac{1}{s}J_n(sa)\sin(bs)ds=\begin{cases}\dfrac{\sin\left[n\sin^{-1}(b/a)\right]}{n}, & a\ge b\\ \dfrac{a^n\sin(n\pi/2)}{n\left[b+\sqrt{b^2-a^2}\right]^n}, & b\ge a\end{cases} \tag{39}$$

$$\int_0^{\infty}\frac{1}{s}J_n(sa)\cos(bs)ds=\begin{cases}\dfrac{\cos\left[n\sin^{-1}(b/a)\right]}{n}, & a\ge b\\ \dfrac{a^n\cos(n\pi/2)}{n\left[b+\sqrt{b^2-a^2}\right]^n}, & b\ge a\end{cases} \tag{40}$$

the semi-infinite integral in Eqs. (37) and (38) can be modified as:

$$\begin{aligned}\int_{-\infty}^{\infty}\frac{d_j(s)}{s^2}J_{n+1}(sl)\left[e^{-isx}-e^{isl}\right]ds=&\begin{cases}\dfrac{2\delta_j}{n+1}\cos\left[(n+1)\sin^{-1}\left(\dfrac{x}{l}\right)\right], & n=0,2,4,6,\ldots\\ \dfrac{-2i\delta_j}{n+1}\sin\left[(n+1)\sin^{-1}\left(\dfrac{x}{l}\right)\right], & n=1,3,5,7,\ldots\end{cases}\\ &+\int_{-\infty}^{\infty}\frac{1}{s}\left[\frac{d_j(s)}{s}-\delta_j\right]J_{n+1}(sl)\left[e^{-isx}-e^{isl}\right]ds \quad (j=1,4)\end{aligned} \tag{41}$$

$$\begin{aligned}\int_{-\infty}^{\infty}\frac{d_j(s)}{s^2}J_{n+1}(sl)\left[e^{-isx}-e^{isl}\right]ds=&\begin{cases}\dfrac{2\delta_j}{n+1}\left\{\cos\left[(n+1)\sin^{-1}\left(\dfrac{x}{l}\right)\right]-(-1)^{\frac{n+1}{2}}\right\}, & n=1,3,5,7,\ldots\\ \dfrac{-2i\delta_j}{n+1}\left\{\sin\left[(n+1)\sin^{-1}\left(\dfrac{x}{l}\right)\right]+(-1)^{\frac{n}{2}}\right\}, & n=0,2,4,6,\ldots\end{cases}\\ &+\int_{0}^{\infty}\frac{1}{s}\left[\frac{d_j(s)}{s}-\delta_j\right]J_{n+1}(sl)\left[e^{-isx}-e^{isl}\right]ds\\ &+\int_{-\infty}^{0}\frac{1}{s}\left[\frac{d_j(s)}{s}+\delta_j\right]J_{n+1}(sl)\left[e^{-isx}-e^{isl}\right]ds \quad (j=2,3)\end{aligned} \tag{42}$$

where $\lim_{s\to\pm\infty} d_1(s)/s=\delta_1$, $\lim_{s\to+\infty} d_2(s)/s=-\lim_{s\to-\infty} d_2(s)/s=\delta_2$, $\lim_{s\to+\infty} d_3(s)/s=-\lim_{s\to-\infty} d_3(s)/s=\delta_3$, $\lim_{s\to\pm\infty} d_4(s)/s=\delta_4$.

It can be seen as follows:

$$\left[\tilde{X}_1\right]=\begin{bmatrix}\mu_{120}^{(1)}\left[-ic_{12}^{(1)}-c_{22}^{(1)}\tilde{m}_1\tilde{\lambda}_1\right] & \mu_{120}^{(1)}\left[-ic_{12}^{(1)}-c_{22}^{(1)}\tilde{m}_2\tilde{\lambda}_2\right]\\ \mu_{120}^{(1)}\left[-\tilde{\lambda}_1-i\tilde{m}_1\right] & \mu_{120}^{(1)}\left[-\tilde{\lambda}_2-i\tilde{m}_2\right]\end{bmatrix} \tag{43}$$

$$\left[\tilde{X}_2\right]=\begin{bmatrix}\mu_{120}^{(2)}\left[-ic_{12}^{(2)}-c_{22}^{(2)}\tilde{m}_3\tilde{\lambda}_3\right] & \mu_{120}^{(2)}\left[-ic_{12}^{(2)}-c_{22}^{(2)}\tilde{m}_4\tilde{\lambda}_4\right]\\ \mu_{120}^{(2)}\left[-\tilde{\lambda}_3-i\tilde{m}_3\right] & \mu_{120}^{(2)}\left[-\tilde{\lambda}_4-i\tilde{m}_4\right]\end{bmatrix} \tag{44}$$

$$\left[\tilde{X}_3\right]=\begin{bmatrix}1 & 1\\ \tilde{m}_1 & \tilde{m}_2\end{bmatrix},\quad \left[\tilde{X}_4\right]=\begin{bmatrix}1 & 1\\ \tilde{m}_3 & \tilde{m}_4\end{bmatrix} \tag{45}$$

$$\left[\tilde{X}_5\right]=\left[\tilde{X}_3\right]-\left[\tilde{X}_4\right]\left[\tilde{X}_2\right]^{-1}\left[\tilde{X}_1\right],\quad \begin{bmatrix}\delta_1 & \delta_2\\ \delta_3 & \delta_4\end{bmatrix}=\left[\tilde{X}_1\right]\left[\tilde{X}_5\right]^{-1} \tag{46}$$

Where

$$\tilde{\lambda}_1=\lim_{s\to+\infty}\lambda_1(s)/s=\sqrt{\frac{-c_{12}^{(1)}\left(2+c_{12}^{(1)}\right)+c_{11}^{(1)}c_{22}^{(1)}+\sqrt{-4c_{11}^{(1)}c_{22}^{(1)}+\left[c_{12}^{(1)}\left(2+c_{12}^{(1)}\right)-c_{11}^{(1)}c_{22}^{(1)}\right]^2}}{2c_{22}^{(1)}}},$$

$$\tilde{\lambda}_2=\lim_{s\to+\infty}\lambda_2(s)/s=\sqrt{\frac{-c_{12}^{(1)}\left(2+c_{12}^{(1)}\right)+c_{11}^{(1)}c_{22}^{(1)}-\sqrt{-4c_{11}^{(1)}c_{22}^{(1)}+\left[c_{12}^{(1)}\left(2+c_{12}^{(1)}\right)-c_{11}^{(1)}c_{22}^{(1)}\right]^2}}{2c_{22}^{(1)}}},$$

$$\tilde{\lambda}_3=\lim_{s\to+\infty}\lambda_3(s)/s=-\sqrt{\frac{-c_{12}^{(2)}\left(2+c_{12}^{(2)}\right)+c_{11}^{(2)}c_{22}^{(2)}+\sqrt{-4c_{11}^{(2)}c_{22}^{(2)}+\left[c_{12}^{(2)}\left(2+c_{12}^{(2)}\right)-c_{11}^{(2)}c_{22}^{(2)}\right]^2}}{2c_{22}^{(2)}}},$$

$$\tilde{\lambda}_4=\lim_{s\to+\infty}\lambda_4(s)/s=-\sqrt{\frac{-c_{12}^{(2)}\left(2+c_{12}^{(2)}\right)+c_{11}^{(2)}c_{22}^{(2)}-\sqrt{-4c_{11}^{(2)}c_{22}^{(2)}+\left[c_{12}^{(2)}\left(2+c_{12}^{(2)}\right)-c_{11}^{(2)}c_{22}^{(2)}\right]^2}}{2c_{22}^{(2)}}},$$

$$\tilde{m}_j=\lim_{s\to+\infty}m_j(s)=\frac{-c_{11}^{(j)}+\tilde{\lambda}_j^2}{-i\tilde{\lambda}_j\left(1+c_{12}^{(j)}\right)}\quad (j=1,2,3,4).$$

When $\mu_{120}^{(1)}=\mu_{120}^{(2)}$, $c_{12}^{(1)}=c_{12}^{(2)}$, $c_{22}^{(1)}=c_{22}^{(2)}$ and $c_{11}^{(1)}=c_{11}^{(2)}$, it can be obtained that $\delta_1=\delta_4=0$,

$$\delta_2=\frac{\mu_{120}^{(1)}\left[2\alpha_1\alpha_2\left(1+c_{12}^{(1)}\right)c_{22}^{(1)}\theta_1-c_{12}^{(1)}\left(-4c_{11}^{(1)}c_{22}^{(1)}+\theta_2^2-\Delta_0^2\right)\right]}{4\sqrt{2}c_{11}^{(1)}c_{22}^{(1)}\left(1+c_{12}^{(1)}\right)(\alpha_1+\alpha_2)} \tag{47}$$

$$\delta_3=\frac{\mu_{120}^{(1)}\left[2\alpha_1\alpha_2\left(1+c_{12}^{(1)}\right)c_{22}^{(1)}\theta_1-c_{12}^{(1)}\left(-4c_{11}^{(1)}c_{22}^{(1)}+\theta_2^2-\Delta_0^2\right)\right]}{2\sqrt{2}c_{22}^{(1)}\left(1+c_{12}^{(1)}\right)\left[\alpha_2(\theta_2+\Delta_0)-\alpha_1(-\theta_2+\Delta_0)\right]} \tag{48}$$

$\theta_1=c_{12}^{(1)2}-c_{11}^{(1)}c_{22}^{(1)}$, $\theta_2=-c_{12}^{(1)}\left(2+c_{12}^{(1)}\right)+c_{11}^{(1)}c_{22}^{(1)}$, $\Delta_0=\sqrt{-4c_{11}^{(1)}c_{22}^{(1)}+\theta_2^2}$, $\alpha_1=\sqrt{\dfrac{\theta_2+\Delta_0}{c_{22}^{(1)}}}$, $\alpha_2=\sqrt{\dfrac{\theta_2-\Delta_0}{c_{22}^{(1)}}}$. This is the same case as in Ref. (13).

The semi-infinite integral in Eqs. (41) and (42) can be evaluated directly. Equations (37) and (38) can now be solved for the coefficients a_n and b_n by the Schmidt method[(14), (15)]. For brevity, Eqs. (37) and (38) can be rewritten as

$$\sum_{n=0}^{\infty}a_nE_n^*(x)+\sum_{n=0}^{\infty}b_nF_n^*(x)=U_0(x),\quad 0\le|x|\le l \tag{49}$$

$$\sum_{n=0}^{\infty}a_nG_n^*(x)+\sum_{n=0}^{\infty}b_nH_n^*(x)=V_0(x),\quad 0\le|x|\le l \tag{50}$$

where $E_n^*(x)$, $F_n^*(x)$, $G_n^*(x)$, $H_n^*(x)$, $U_0(x)$ and $V_0(x)$ are known functions. The coefficients a_n and b_n are unknown.

From Eq. (50), it can be obtained:

$$\sum_{n=0}^{\infty}b_nH_n^*(x)=-\sum_{n=0}^{\infty}a_nG_n^*(x)+V_0(x) \tag{51}$$

It can now be solved for the coefficients b_n by the Schmidt method[(14), (15), (23)–(28)]. Here the form $-\sum_{n=0}^{\infty}a_nG_n^*(x)+V_0(x)$ can be considered as a known function temporarily. A set of functions $P_n(x)$, which satisfy the orthogonality condition

$$\int_{-l}^{l}P_m(x)P_n(x)dx=N_n\delta_{mn},\quad N_n=\int_{-l}^{l}P_n^2(x)dx \tag{52}$$

can be constructed from the function, $H_n^*(x)$, such that

$$P_n(x)=\sum_{i=0}^{n}\frac{M_{in}}{M_{nn}}H_i^*(x) \tag{53}$$

where M_{ij} is the cofactor of the element d_{ij} of D_n, which is defined as

$$D_n=\begin{bmatrix}d_{00},d_{01},d_{02},\ldots,d_{0n}\\ d_{10},d_{11},d_{12},\ldots,d_{1n}\\ d_{20},d_{21},d_{22},\ldots,d_{2n}\\ \cdots\cdots\cdots\cdots\cdots\\ \cdots\cdots\cdots\cdots\cdots\\ \cdots\cdots\cdots\cdots\cdots\\ d_{n0},d_{n1},d_{n2},\ldots,d_{nn}\end{bmatrix},\quad d_{ij}=\int_{-l}^{l}H_i^*(x)H_j^*(x)dx \tag{54}$$

Using Eqs. (51) – (54), it can be obtained that

$$b_n=\sum_{j=n}^{\infty}q_j\frac{M_{nj}}{M_{jj}}\ \text{with}$$

$$q_j = -\sum_{i=0}^{\infty} a_i \frac{1}{N_j} \int_{-l}^{l} G_i^*(x) P_j(x) dx + \frac{1}{N_j} \int_{-l}^{l} V_0(x) P_j(x) dx \tag{55}$$

So it can be rewritten

$$b_n = \sum_{i=0}^{\infty} a_i K_{in}^* + \sum_{j=n}^{\infty} \frac{M_{nj}}{N_j M_{jj}} \int_{-l}^{l} V_0(x) P_j(x) dx,$$

$$K_{in}^* = -\sum_{j=n}^{\infty} \frac{M_{nj}}{N_j M_{jj}} \int_{-l}^{l} G_i^*(x) P_j(x) dx \tag{56}$$

Substituting Eq. (56) into Eq. (49), it can be obtained

$$\sum_{n=0}^{\infty} a_n Y_n^*(x) = U_0(x) - W(x),$$

$$Y_n^*(x) = E_n^*(x) + \sum_{i=0}^{\infty} K_{ni}^* F_i^*(x),$$

$$W(x) = \sum_{n=0}^{\infty} F_n(x) \sum_{j=n}^{\infty} \frac{M_{nj}}{N_j M_{jj}} \int_{-l}^{l} V_0(s) P_j(s) ds \tag{57}$$

So it can now be solved for the coefficients a_n by the Schmidt method again as mentioned above. With the aid of Eq. (56), the coefficients b_n can be obtained.

5. Stress Intensity Factors

The coefficients a_n and b_n are known, so that the entire stress field can be obtained. However, in fracture mechanics, it is important to determine stresses $\sigma_y^{(1)}$ and $\tau_{xy}^{(1)}$ in the vicinity of the crack tips. In the case of the present study, $\sigma_y^{(1)}$ and $\tau_{xy}^{(1)}$ along the crack line can be expressed as:

$$\begin{aligned}
&\sigma_y^{(1)}(x,0) \\
&= \frac{e^{\beta x}}{2\pi} \sum_{n=0}^{\infty} G_n \int_{-\infty}^{\infty} \frac{1}{s} [d_1(s) a_n + d_2(s) b_n] J_{n+1}(sl) e^{-isx} ds \\
&= \frac{e^{\beta x}}{2\pi} \sum_{n=0}^{\infty} G_n \Bigg\{ a_n \int_{-\infty}^{\infty} \left(\frac{d_1(s)}{s} - \delta_1 \right) J_{n+1}(sl) e^{-isx} ds \\
&\quad + b_n \int_{0}^{\infty} \left(\frac{d_2(s)}{s} - \delta_2 \right) J_{n+1}(sl) e^{-isx} ds \\
&\quad + b_n \int_{-\infty}^{0} \left(\frac{d_2(s)}{s} + \delta_2 \right) J_{n+1}(sl) e^{-isx} ds \\
&\quad + \delta_1 a_n \int_{-\infty}^{\infty} J_{n+1}(sl) e^{-isx} ds \\
&\quad + \delta_2 b_n \int_{0}^{\infty} J_{n+1}(sl) e^{-isx} ds \\
&\quad - \delta_2 b_n \int_{-\infty}^{0} J_{n+1}(sl) e^{-isx} ds \Bigg\}
\end{aligned} \tag{58}$$

$$\begin{aligned}
&\tau_{xy}^{(1)}(x,0) \\
&= \frac{e^{\beta x}}{2\pi} \sum_{n=0}^{\infty} G_n \int_{-\infty}^{\infty} \frac{1}{s} [d_3(s) a_n + d_4(s) b_n] J_{n+1}(sl) e^{-isx} ds \\
&= \frac{e^{\beta x}}{2\pi} \sum_{n=0}^{\infty} G_n \Bigg\{ a_n \int_{0}^{\infty} \left(\frac{d_3(s)}{s} - \delta_3 \right) J_{n+1}(sl) e^{-isx} ds \\
&\quad + a_n \int_{-\infty}^{0} \left(\frac{d_3(s)}{s} + \delta_3 \right) J_{n+1}(sl) e^{-isx} ds \\
&\quad + b_n \int_{-\infty}^{\infty} \left(\frac{d_4(s)}{s} - \delta_4 \right) J_{n+1}(sl) e^{-isx} ds \\
&\quad + \delta_3 a_n \int_{0}^{\infty} J_{n+1}(sl) e^{-isx} ds \\
&\quad - \delta_3 a_n \int_{-\infty}^{0} J_{n+1}(sl) e^{-isx} ds \\
&\quad + \delta_4 b_n \int_{-\infty}^{\infty} J_{n+1}(sl) e^{-isx} ds \Bigg\}
\end{aligned} \tag{59}$$

An examination of Eqs. (58) and (59) shows that, the singular part of the stress field can be obtained from the relationships as follows[21]:

$$\int_0^{\infty} J_n(sa) \cos(bs) ds = \begin{cases} \dfrac{\cos\left[n \sin^{-1}(b/a)\right]}{\sqrt{a^2 - b^2}}, & a > b \\ -\dfrac{a^n \sin(n\pi/2)}{\sqrt{b^2 - a^2}\left[b + \sqrt{b^2 - a^2}\right]^n}, & b > a \end{cases} \tag{60}$$

$$\int_0^{\infty} J_n(sa) \sin(bs) ds = \begin{cases} \dfrac{\sin\left[n \sin^{-1}(b/a)\right]}{\sqrt{a^2 - b^2}}, & a > b \\ \dfrac{a^n \cos(n\pi/2)}{\sqrt{b^2 - a^2}\left[b + \sqrt{b^2 - a^2}\right]^n}, & b > a \end{cases} \tag{61}$$

$$\int_{-\infty}^{\infty} J_{n+1}(sl) e^{-isx} ds = 0, \quad x > l \tag{62}$$

For $l < x$, the singular part of the stress fields can be expressed respectively as follows:

$$\begin{aligned}
\sigma &= \frac{\delta_2 e^{\beta x}}{2\pi} \sum_{n=0}^{\infty} b_n G_n \left[\int_0^{\infty} J_{n+1}(sl) e^{-isx} ds - \int_{-\infty}^{0} J_{n+1}(sl) e^{-isx} ds \right] \\
&= -\frac{\delta_2 e^{\beta x}}{\pi} \sum_{n=0}^{\infty} b_n G_n Q_n(x)
\end{aligned} \tag{63}$$

$$\begin{aligned}
\tau &= \frac{\delta_3 e^{\beta x}}{2\pi} \sum_{n=0}^{\infty} a_n G_n \left[\int_0^{\infty} J_{n+1}(sl) e^{-isx} ds - \int_{-\infty}^{0} J_{n+1}(sl) e^{-isx} ds \right] \\
&= -\frac{\delta_3 e^{\beta x}}{\pi} \sum_{n=0}^{\infty} a_n G_n Q_n(x)
\end{aligned} \tag{64}$$

where

$$Q_n(x) = \begin{cases} \dfrac{(-1)^{\frac{n}{2}} l^{n+1}}{\sqrt{x^2 - l^2}\left[x + \sqrt{x^2 - l^2}\right]^{n+1}}, & n = 0, 2, 4, 6, \ldots \\ \dfrac{i(-1)^{\frac{n+1}{2}} l^{n+1}}{\sqrt{x^2 - l^2}\left[x + \sqrt{x^2 - l^2}\right]^{n+1}}, & n = 1, 3, 5, 7, \ldots \end{cases}$$

For $x < -l$, the singular part of the stress fields can be expressed respectively as follows:

$$\sigma = \frac{\delta_2 e^{\beta x}}{2\pi}\sum_{n=0}^{\infty} b_n G_n\left[\int_0^{\infty} J_{n+1}(sl)e^{-isx}ds - \int_{-\infty}^{0} J_{n+1}(sl)e^{-isx}ds\right]$$
$$= -\frac{\delta_2 e^{\beta x}}{\pi}\sum_{n=0}^{\infty} b_n G_n Q_n^*(x) \tag{65}$$

$$\tau = \frac{\delta_3 e^{\beta x}}{2\pi}\sum_{n=0}^{\infty} a_n G_n\left[\int_0^{\infty} J_{n+1}(sl)e^{-isx}ds - \int_{-\infty}^{0} J_{n+1}(sl)e^{-isx}ds\right]$$
$$= -\frac{\delta_3 e^{\beta x}}{\pi}\sum_{n=0}^{\infty} a_n G_n Q_n^*(x) \tag{66}$$

where

$$Q_n^*(x) = \begin{cases} \dfrac{(-1)^{\frac{n}{2}} l^{n+1}}{\sqrt{x^2-l^2}\left[|x| + \sqrt{x^2-l^2}\right]^{n+1}}, & n = 0,2,4,6,\dots \\[2ex] \dfrac{-i(-1)^{\frac{n+1}{2}} l^{n+1}}{\sqrt{x^2-l^2}\left[|x| + \sqrt{x^2-l^2}\right]^{n+1}}, & n = 1,3,5,7,\dots \end{cases}$$

The values of the stress intensity factor at the right tip of the crack can be given as follows

$$K_{\mathrm{I}}(l) = \lim_{x\to l^+}\sqrt{2(x-l)}\cdot\sigma$$
$$= -\frac{2\delta_2 e^{\beta l}}{\sqrt{\pi l}}\sum_{n=0}^{\infty}(-1)^n b_n \frac{\Gamma\left(n+1+\frac{1}{2}\right)}{n!} \tag{67}$$

$$K_{\mathrm{II}}(l) = \lim_{x\to l^+}\sqrt{2(x-l)}\cdot\tau$$
$$= -\frac{2\delta_3 e^{\beta l}}{\sqrt{\pi l}}\sum_{n=0}^{\infty}(-1)^n a_n \frac{\Gamma\left(n+1+\frac{1}{2}\right)}{n!} \tag{68}$$

The values of the stress intensity factor at the left tip of the crack can be given as follows

$$K_{\mathrm{I}}(-l) = \lim_{x\to -l^-}\sqrt{2(|x|-l)}\cdot\sigma$$
$$= -\frac{2\delta_2 e^{-\beta l}}{\sqrt{\pi l}}\sum_{n=0}^{\infty} b_n \frac{\Gamma\left(n+1+\frac{1}{2}\right)}{n!} \tag{69}$$

$$K_{\mathrm{II}}(-l) = \lim_{x\to -l^-}\sqrt{2(|x|-l)}\cdot\tau$$
$$= -\frac{2\delta_3 e^{-\beta l}}{\sqrt{\pi l}}\sum_{n=0}^{\infty} a_n \frac{\Gamma\left(n+1+\frac{1}{2}\right)}{n!} \tag{70}$$

Table 1 Values of $\left[\sum_{n=0}^{9} a_n E_n^*(x) + \sum_{n=0}^{9} b_n F_n^*(x)\right]\Big/(2\pi\sigma_0)$ and $U_0(x)/\sigma_0$ for $\beta l = 0.1$, $-\sigma_0(x) = -p_0$, $\tau_0(x) = 0.0$, $\mu_{120}^{(1)} = \mu_{120}^{(2)} = 6.4\,\mathrm{GPa}$, $E_{10}^{(1)} = E_{10}^{(2)} = 207.0\,\mathrm{GPa}$, $E_{20}^{(1)} = E_{20}^{(2)} = 19.0\,\mathrm{GPa}$ and $\nu_{12}^{(1)} = \nu_{23}^{(1)} = \nu_{12}^{(2)} = \nu_{23}^{(2)} = 0.21$

x	$[\sum_{n=0}^{9} a_n E_n^*(x) + \sum_{n=0}^{9} b_n F_n^*(x)]/(2\pi\sigma_0)$		$U_0(x)/\sigma_0$
	Real part	Imaginary part	
0.08	-0.335950D+00	0.634354D-06	-0.336014D+00
0.12	-0.336352D+00	0.654894D-06	-0.336419D+00
0.20	-0.338435D+00	0.643771D-06	-0.338506D+00
0.24	-0.340369D+00	0.836626D-06	-0.340443D+00
0.32	-0.346661D+00	0.670968D-06	-0.346740D+00
0.40	-0.357030D+00	0.812209D-06	-0.357113D+00
0.52	-0.382440D+00	0.971902D-06	-0.382530D+00
0.60	-0.407425D+00	0.111449D-05	-0.407520D+00
0.72	-0.459487D+00	0.121751D-05	-0.459589D+00
0.80	-0.505382D+00	0.130893D-05	-0.505489D+00
0.88	-0.561395D+00	0.118526D-05	-0.561507D+00
0.92	-0.593508D+00	0.112408D-05	-0.593622D+00
0.96	-0.628524D+00	0.117726D-05	-0.628640D+00

Table 2 Values of a_n and b_n for $\beta l = 0.1$, $-\sigma_0(x) = -p_0$, $\tau_0(x) = 0.0$, $\mu_{120}^{(1)} = \mu_{120}^{(2)} = 6.4\,\mathrm{GPa}$, $E_{10}^{(1)} = E_{10}^{(2)} = 207.0\,\mathrm{GPa}$, $E_{20}^{(1)} = E_{20}^{(2)} = 19.0\,\mathrm{GPa}$ and $\nu_{12}^{(1)} = \nu_{23}^{(1)} = \nu_{12}^{(2)} = \nu_{23}^{(2)} = 0.21$

n	$a_n/(2\pi\sigma_0)$		$b_n/(2\pi\sigma_0)$	
	Real part	Imaginary part	Real part	Imaginary part
0	0.945628D-02	-0.821088D-09	0.796148D-05	-0.207069D-10
1	0.447544D-04	0.376669D-09	0.605202D-06	0.165248D-11
2	0.106567D-06	-0.121080D-09	0.424735D-07	-0.693769D-11
3	0.548460D-07	0.457541D-10	0.207524D-08	0.200616D-11
4	0.155097D-07	0.186251D-10	0.508114D-09	0.961863D-12
5	0.433377D-08	0.614823D-11	0.368583D-10	0.177465D-12
6	0.567221D-09	0.331182D-12	0.720552D-11	-0.422709D-13
7	0.231342D-09	0.401144D-12	0.220275D-11	0.105477D-13
8	0.103451D-10	0.331227D-13	0.102215D-11	0.121751D-14
9	0.434138D-11	0.335267D-14	0.543321D-12	0.754752D-16

6. Numerical Calculations and Discussion

To check the numerical accuracy of the Schmidt method, the values of $\left[\sum_{n=0}^{9} a_n E_n^*(x) + \sum_{n=0}^{9} b_n F_n^*(x)\right]\Big/(2\pi\sigma_0)$ and $U_0(x)/\sigma_0$ are given in Table 1 for $\beta l = 0.1$, $-\sigma_0(x) = -p_0$, $\tau_0(x) = 0.0$, $\mu_{120}^{(1)} = \mu_{120}^{(2)} = 6.4\,\mathrm{GPa}$, $E_{10}^{(1)} = E_{10}^{(2)} = 207.0\,\mathrm{GPa}$, $E_{20}^{(1)} = E_{20}^{(2)} = 19.0\,\mathrm{GPa}$ and $\nu_{12}^{(1)} = \nu_{23}^{(1)} = \nu_{12}^{(2)} = \nu_{23}^{(2)} = 0.21$. In Table 2, the values of the coefficients a_n and b_n are given for $\beta l = 0.1$, $-\sigma_0(x) = -p_0$, $\tau_0(x) = 0.0$, $\mu_{120}^{(1)} = \mu_{120}^{(2)} = 6.4\,\mathrm{GPa}$, $E_{10}^{(1)} = E_{10}^{(2)} = 207.0\,\mathrm{GPa}$, $E_{20}^{(1)} = E_{20}^{(2)} = 19.0\,\mathrm{GPa}$ and $\nu_{12}^{(1)} = \nu_{23}^{(1)} = \nu_{12}^{(2)} = \nu_{23}^{(2)} = 0.21$.

As discussed in the works[(23)-(28)] and the above discussion, it can be seen that the Schmidt method is performed satisfactorily if the first ten terms of infinite series in Eqs. (31) and (33) are retained. The behavior of the sum of the series keeps steady with the increasing number of terms in Eqs. (31) and (33). For the case in which the material properties are not continuous along the interface, it is assumed that $\left(\mu_{120}^{(1)}, E_{10}^{(1)}, E_{20}^{(1)}, \nu_{12}^{(1)}, \nu_{23}^{(1)}\right) = (7.07\,\mathrm{GPa}, 156.75\,\mathrm{GPa}, 10.41\,\mathrm{GPa}, 0.31, 0.49)$ and $(\mu_{120}^{(2)}, E_{10}^{(2)}, E_{20}^{(2)}, \nu_{12}^{(2)}, \nu_{23}^{(2)}) = (6.4\,\mathrm{GPa}, 207\,\mathrm{GPa}, 19\,\mathrm{GPa}, 0.21, 0.21)$. For the case in which the material properties are continuous along the interface, it is assumed that $\left(\mu_{120}^{(1)}, E_{10}^{(1)}, E_{20}^{(1)}, \nu_{12}^{(1)}, \nu_{23}^{(1)}\right) = \left(\mu_{120}^{(2)}, E_{10}^{(2)}, E_{20}^{(2)}, \nu_{12}^{(2)}, \nu_{23}^{(2)}\right) = (7.07\,\mathrm{GPa}, 156.75\,\mathrm{GPa}, 10.41\,\mathrm{GPa}, 0.31, 0.49)$. The crack surface loading $-\sigma_0(x)$ and $-\tau_0(x)$ will simply be assumed to be a polynomial of the form as follows:

$$-\sigma_0(x) = -p_0 - p_1\left(\frac{x}{l}\right) - p_2\left(\frac{x}{l}\right)^2 - p_3\left(\frac{x}{l}\right)^3$$

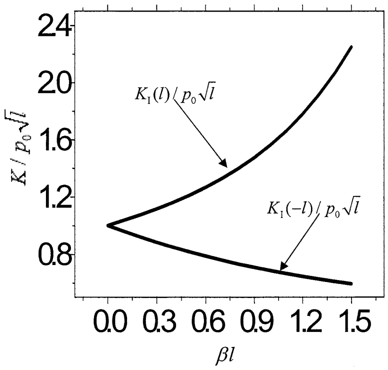

Fig. 2 Influence of βl on the normalized Mode-I SIFs under the loading $\sigma_0(x)=p_0$ and $\tau_0(x)=0$ for the case in which the properties are continuous along the crack line

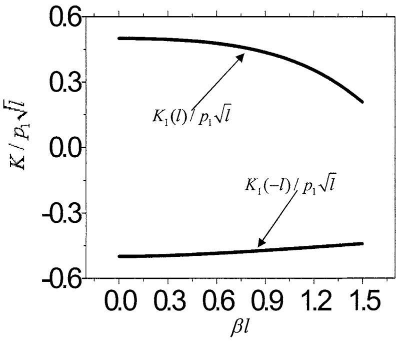

Fig. 3 Influence of βl on the normalized Mode-I SIFs under the loading $\sigma_0(x)=p_1\left(\frac{x}{l}\right)$ and $\tau_0(x)=0$ for the case in which the properties are continuous along the crack line

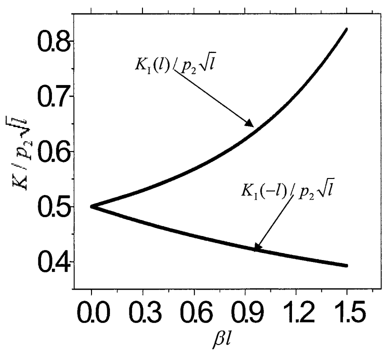

Fig. 4 Influence of βl on the normalized Mode-I SIFs under the loading $\sigma_0(x)=p_2\left(\frac{x}{l}\right)^2$ and $\tau_0(x)=0$ for the case in which the properties are continuous along the crack line

$$-\tau_0(x)=-s_0-s_1\left(\frac{x}{l}\right)-s_2\left(\frac{x}{l}\right)^2-s_3\left(\frac{x}{l}\right)^3$$

Since the problem is linear, the results can be superimposed in any suitable manner. The results are obtained by taking only one or two of the eight input parameters p_0, p_1, p_2, p_3, s_0, s_1, s_2 and s_3 nonzero at a time. The values of the stress intensity factor are calculated numerically. The results of the present paper are shown in Fig. 2 to Fig. 11.

From the results, the following observations can be made:

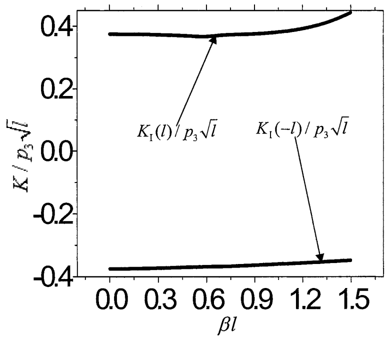

Fig. 5 Influence of βl on the normalized Mode-I SIFs under the loading $\sigma_0(x)=p_3\left(\frac{x}{l}\right)^3$ and $\tau_0(x)=0$ for the case in which the properties are continuous along the crack line

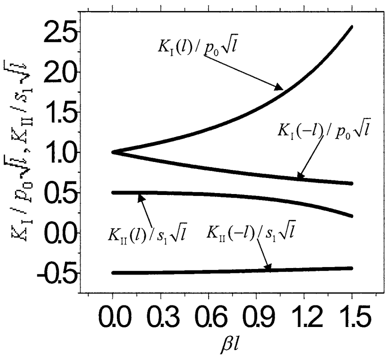

Fig. 6 Influence of βl on the values of the stress intensity factor K under the loading $\sigma_0(x)=p_0$ and $\tau_0(x)=s_1\left(\frac{x}{l}\right)$ for the case in which the properties are continuous along the crack line

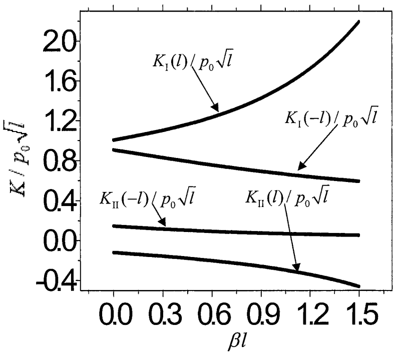

Fig. 7 Influence of βl on the normalized Mode-I SIFs under the loading $\sigma_0(x)=p_0$ and $\tau_0(x)=0$ for the case in which the properties are not continuous along the crack line

(i) The aim of the present paper is to give a new approach to solve the same problem as in Ref. (13). The solving process is quite different from the other works such as in Refs. (13) and (16)–(20). The results are similar to that in Ref. (13) as shown in Table 3 and Fig. 2 when $\left(\mu_{120}^{(1)},E_{10}^{(1)},E_{20}^{(1)},\nu_{12}^{(1)},\nu_{23}^{(1)}\right)=\left(\mu_{120}^{(2)},E_{10}^{(2)},E_{20}^{(2)},\nu_{12}^{(2)},\nu_{23}^{(2)}\right)$. It is also proved that the Schmidt method is performed satisfactorily. Further more, the numerical solutions are obtained when the material properties are not continuous

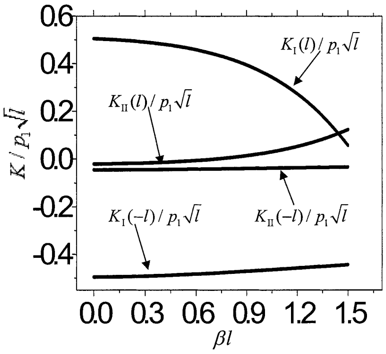

Fig. 8 Influence of βl on the values of the stress intensity factor K under the loading $\sigma_0(x) = p_1\left(\frac{x}{l}\right)$ and $\tau_0(x) = 0$ for the case in which the properties are not continuous along the crack line

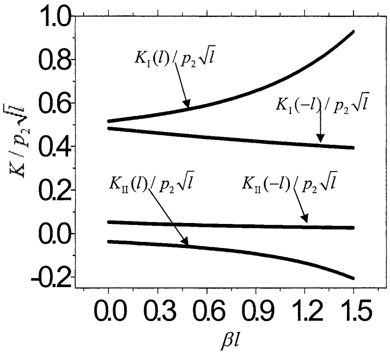

Fig. 9 Influence of βl on the normalized Mode-I SIFs under the loading $\sigma_0(x) = p_2\left(\frac{x}{l}\right)^2$ and $\tau_0(x) = 0$ for the case in which the properties are not continuous along the crack line

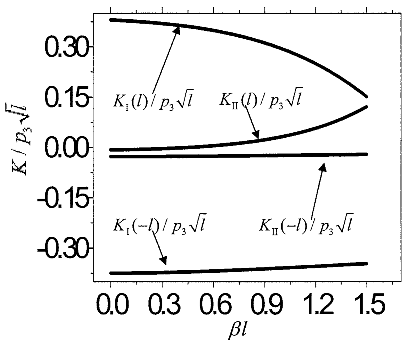

Fig. 10 Influence of βl on the normalized Mode-I SIFs under the loading $\sigma_0(x) = p_3\left(\frac{x}{l}\right)^3$ and $\tau_0(x) = 0$ for the case in which the properties are not continuous along the crack line

across the crack line under the assumptions that the effect of the crack surface overlapping very near the crack tips is negligible. For this special case (From practical view points, researchers in the field of functionally graded materials will not pay their attention in this case), it is found that the stress singularities of the present interface crack solution are similar to ones for the ordinary crack in ho-

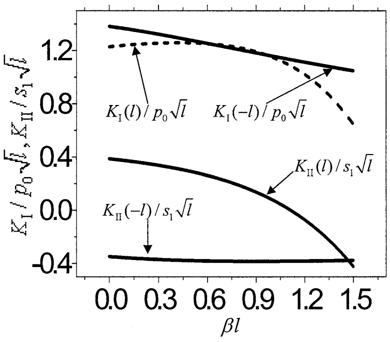

Fig. 11 Influence of βl on the values of the stress intensity factor K under the loading $\sigma_0(x) = p_0$ and $\tau_0(x) = s_1\left(\frac{x}{l}\right)$ for the case in which the properties are not continuous along the crack line

Table 3 The normalized stress intensity factors for an inhomogeneous orthotropic medium under crack loading $\sigma_0(x) = p_0$ and $\tau_0(x) = 0$ for the case $k = 5.0$ and $\nu = 0.3$ when the material properties are continuous along the crack line. Where $k = \frac{E^{(1)}}{2\mu_{120}^{(1)}} - \nu$, $\nu = \sqrt{\nu_{12}^{(1)}\nu_{21}^{(1)}}$, $E^{(1)} = \sqrt{E_{10}^{(1)}E_{20}^{(1)}}$

βl	$K_I^*(l)/p_0\sqrt{l}$	$K_I^*(-l)/p_0\sqrt{l}$	$K_I(l)/p_0\sqrt{l}$	$K_I(-l)/p_0\sqrt{l}$
0.00	1.0	1.0	1.0	1.0
0.01	1.0025	0.9975	1.00281	0.997158
0.10	1.0231	0.9733	1.02695	0.970557
0.25	1.0631	0.9306	1.06424	0.924860
0.50	1.0946	0.8594	1.12293	0.851615
0.75	1.1281	0.7932	1.18009	0.785286
1.00	1.1556	0.7339	1.23760	0.726810
1.50	1.1979	0.6367	1.35615	0.631754
2.00	1.2290	0.5636	1.45838	0.560195

Where $K_I^*(l)/p_0\sqrt{l}$ and $K_I^*(-l)/p_0\sqrt{l}$ represent the stress intensity factors in Ref. (13).

mogeneous orthotropic materials(16), (17). This special case was not considered in Ref. (13).

(ii) In the present paper, the unknown variables of dual integral equations are the displacement across the crack surfaces. However, in the previous works(13), (16)-(20), the unknown variables of dual integral equations are the dislocation density functions. During the solution process in the present paper, the results can be directly obtained, without any need to solve the singular integral equations. This is the major difference.

(iii) It can be obtained that the values of the shear stress intensity factors are equal to zero for the tension loading $\sigma_0(x) = p_0$ and $\tau_0(x) = 0$ when $\left(\mu_{120}^{(1)}, E_{10}^{(1)}, E_{20}^{(1)}, \nu_{12}^{(1)}, \nu_{23}^{(1)}\right) = \left(\mu_{120}^{(2)}, E_{10}^{(2)}, E_{20}^{(2)}, \nu_{12}^{(2)}, \nu_{23}^{(2)}\right)$ from the results as shown in Fig. 2 to Fig. 5. However, it can be obtained that the shear stress intensity factors are not equal to zero for the tension loading $\sigma_0(x) = p_0$ and $\tau_0(x) = 0$, the normal stress intensity factors are also not equal to zero for the shear loading $\tau_0(x) = s_1\left(\frac{x}{l}\right)$ and $\sigma_0(x) =$

0 when $\left(\mu_{120}^{(1)}, E_{10}^{(1)}, E_{20}^{(1)}, \nu_{12}^{(1)}, \nu_{23}^{(1)}\right) \neq \left(\mu_{120}^{(2)}, E_{10}^{(2)}, E_{20}^{(2)}, \nu_{12}^{(2)}, \nu_{23}^{(2)}\right)$ as shown in Fig. 7 to Fig. 11. This is consistent with the results in Refs. (29) and (30).

(iv) It can be obtained that the stress intensity factors $K_{\mathrm{I}}(l)/p_0\sqrt{l} = K_{\mathrm{I}}(-l)/p_0\sqrt{l} = 1.0$ under the tension loading $\sigma_0(x) = p_0$ and $\tau_0(x) = 0$ for $\beta l = 0$ and $\left(\mu_{120}^{(1)}, E_{10}^{(1)}, E_{20}^{(1)}, \nu_{12}^{(1)}, \nu_{23}^{(1)}\right) = \left(\mu_{120}^{(2)}, E_{10}^{(2)}, E_{20}^{(2)}, \nu_{12}^{(2)}, \nu_{23}^{(2)}\right)$. However, it can be obtained that the stress intensity factors $K_{\mathrm{I}}(l)/p_0\sqrt{l}$ and $K_{\mathrm{I}}(-l)/p_0\sqrt{l}$ tend to unit under the tension loading $\sigma_0(x) = p_0$ and $\tau_0(x) = 0$ for $\beta l = 0$ and $\left(\mu_{120}^{(1)}, E_{10}^{(1)}, E_{20}^{(1)}, \nu_{12}^{(1)}, \nu_{23}^{(1)}\right) \neq \left(\mu_{120}^{(2)}, E_{10}^{(2)}, E_{20}^{(2)}, \nu_{12}^{(2)}, \nu_{23}^{(2)}\right)$ as shown in Figs. 2 and 7.

(v) From the results, it can be obtained that the Schmidt method can be used to solve the mix boundary crack problem as shown in Figs. 6 and 11.

(vi) The influence of the normalized non-homogeneity constant βl on the stress fields is quite significant. It can be obtained that the stress intensity factor $K_{\mathrm{I}}(l)/p_0\sqrt{l}$ tends to increase with increase in the normalized non-homogeneity constant βl, the stress intensity factor $K_{\mathrm{I}}(-l)/p_0\sqrt{l}$ tends to decrease with increase in the normalized non-homogeneity constant βl as shown in Figs. 2 and 7 for the tension loading $\sigma_0(x) = p_0$ and $\tau_0(x) = 0$.

(vii) It can be obtained that the stress intensity factor $K_{\mathrm{I}}(l)/p_1\sqrt{l}$ tends to decrease with increase in the normalized non-homogeneity constant βl, the stress intensity factor $K_{\mathrm{I}}(-l)/p_1\sqrt{l}$ changes slowly with increase in the normalized non-homogeneity constant βl as shown in Figs. 3 and 8 for the tension loading $\sigma_0(x) = p_1\left(\frac{x}{l}\right)$ and $\tau_0(x) = 0$. It can be also obtained that $K_{\mathrm{I}}(l)/p_1\sqrt{l} = 0.5$ and $K_{\mathrm{I}}(-l)/p_1\sqrt{l} = -0.5$ for $\beta l = 0$ under the tension loading $\sigma_0(x) = p_1\left(\frac{x}{l}\right)$ and $\tau_0(x) = 0$.

Acknowledgements

The authors are grateful for the financial support by the Natural Science Foundation of Hei Long Jiang Province (A0301), the National Natural Science Foundation of China (50232030, 10172030) and the Foundation of Space Innovation of China.

References

(1) Koizumi, M., The Concept of FGM, edited by Holt, J.B., et al., Ceramic Transactions, Vol.34, (1993), pp.3–10, Functionally Graded Materials, American Ceramic Society, Ohio.

(2) Lee, Y.D. and Erdogan, F., Residual/Thermal Stress in FGM and Laminated Thermal Barrier Coating, International Journal of Fracture, Vol.69 (1994), pp.145–165.

(3) Suresh, S. and Mortensen, A., Functionally Graded Metals and Metal-Ceramic Composites: Part 2 Thermomechanical Behaviour, International Materials Reviews, Vol.29 (1977), pp.306–312.

(4) Choi, H.J., The Problem for Bonded Half-Planes Containing a Crack at an Arbitrary Angle to the Graded Interfacial Zone, International Journal of Solids and Structures, Vol.38 (2001), pp.6559–6588.

(5) Delale, F. and Erdogan, F., On the Mechanical Modeling of the Interfacial Region in Bonded Half-Planes, ASME Journal of Applied Mechanics, Vol.55 (1988), pp.317–324.

(6) Chen, Y.F., Interface Crack in Nonhomogeneous Bonded Materials of Finite Thickness, Ph.D. Dissertation, (1990), Lehigh University.

(7) Ozturk, M. and Erdogan, F., Axisymmetric Crack Problem in Bonded Materials with a Graded Interfacial Region, International Journal of Solids and Structures, Vol.33 (1996), pp.193–219.

(8) Jin, Z.H. and Batra, R.C., Interface Cracking between Functionally Graded Coating and a Substrate under Antiplane Shear, International Journal of Engineering Science, Vol.34 (1996), pp.1705–1716.

(9) Bao, G. and Cai, H., Delamination Cracking in Functionally Graded Coating/Metal Substrate Systems, ACTA Materialia, Vol.45 (1997), pp.1055–1066.

(10) Shbeeb, N.I. and Binienda, W.K., Analysis of an Interface Crack for a Functionally Graded Strip Sandwiched between Two Homogeneous Layers of Finite Thickness, Engineering Fracture Mechanics, Vol.64 (1999), pp.693–720.

(11) Wang, B.L., Han, J.C. and Du, S.Y., Crack Problem for Non-Homogeneous Composite Materials Subjected to Dynamic Loading, International Journal of Solids and Structures, Vol.37 (2000), pp.1251–1274.

(12) Erdogan, F. and Wu, H.B., Crack Problems in FGM Layer under Thermal Stress, Journal of Thermal Stress, Vol.19 (1996), pp.237–265.

(13) Ozturk, M. and Erdogan, F., Mode I Crack Problem in an Inhomogeneous Orthotropic Medium, International Journal of Engineering Science, Vol.35 (1997), pp.869–883.

(14) Morse, P.M. and Feshbach, H., Methods of Theoretical Physics, Vol.1, (1958), p.926, McGraw-Hill, New York.

(15) Itou, S., Three Dimensional Waves Propagation in a Cracked Elastic Solid, ASME Journal of Applied Mechanics, Vol.45 (1978), pp.807–811.

(16) Cai, H.T. and Yuan, X.G., Crack Problem of Two Bonded Half Orthotropic Planes Materials, Engineering Fracture Mechanics, Vol.52, No.5 (1995), pp.895–900.

(17) Matbuly, M.S., Analytical Solution for Crack Problems in Orthotropic Plate Materials, Journal of Engineering and Applied Science, Vol.48, No.6 (2001), pp.1115–1129.

(18) Erdogan, F. and Wu, B.H., Interface Crack Problems in Layered Orthotropic Materials, Journal of the Mechanics and Physics of Solids, Vol.41, No.5 (1993), pp.889–917.

(19) Zhang, X.S., A Central Crack at the Interface between Two Different Orthotropic Media for the Mode I and Mode II, Engineering Fracture Mechanics, Vol.33, No.3 (1989), pp.327–333.

(20) Zhang, X.S., A Center Crack at the Interface between Two Different Media for the Opening Mode, Engineer-

ing Fracture Mechanics, Vol.24, No.2 (1986), pp.177–185.
(21) Gradshteyn, I.S. and Ryzhik, I.M., Table of Integrals, Series and Products, (1980), Academic Press, New York.
(22) Erdelyi, A. (ed.), Tables of Integral Transforms, Vol.1, (1954), McGraw-Hill, New York.
(23) Zhou, Z.G., Bai, Y.Y. and Zhang, X.W., Two Collinear Griffith Cracks Subjected to Uniform Tension in Infinitely Long Strip, International Journal of Solids and Structures, Vol.36 (1999), pp.5597–5609.
(24) Zhou, Z.G., Han, J.C. and Du, S.Y., Investigation of a Griffith Crack Subject to Anti-Plane Shear by Using the Non-Local Theory, International Journal of Solids and Structures, Vol.36 (1999), pp.3891–3901.
(25) Itou, S., Stress Intensity Factors around a Crack in a Non-Homogeneous Interface Layer between Two Dissimilar Elastic Half-Planes, International Journal of Fracture, Vol.110 (2001), pp.123–135.
(26) Zhou, G.Z. and Wang, B., The Scattering of Harmonic Elastic Anti-Plane Shear Waves by a Griffith Crack in a Piezoelectric Material Plane by Using the Non-Local Theory, International Journal of Engineering Science, Vol.40, No.3 (2002), pp.303–317.
(27) Itou, S., Stress Intensity Factors around a Cylindrical Crack in an Interfacial Zone in Composite Materials, International Journal of Solids and Structures, Vol.36 (1999), pp.697–709.
(28) Itou, S., Stresses around an Interface Crack, Engineering Fracture Mechanics, Vol.25 (1986), pp.415–420.
(29) Chen, Y.F. and Erdogan, F., The Interface Crack Problem for a Nonhomogeneous Coating Boended to a Homogeneous Substrate, Journal of Mechanics and Physics of Solids, Vol.44, No.5 (1996), pp.771–787.
(30) England, A.H., A Crack between Dissimilar Media, Journal of Applied Mechanics, Vol.32 (1965), pp.400–402.